**Title:** Structure and soft magnetic properties of Fe72B20Si4Nb4 bulk metallic glasses

**Author:** R. Nowosielski, R. Babilas, S. Griner, Zbigniew Stokłosa

Archives of Materials Science and Engineering

Volume 35
Issue 1
January 2009
Pages 13-20

International Scientific Journal
published monthly by the
World Academy of Materials
and Manufacturing Engineering

# Structure and soft magnetic properties of $Fe_{72}B_{20}Si_4Nb_4$ bulk metallic glasses

**R. Nowosielski [a], R. Babilas [a,*], S. Griner [a], Z. Stokłosa [b]**

[a] Division of Nanocrystalline and Functional Materials and Sustainable Pro-ecological Technologies, Institute of Engineering Materials and Biomaterials, Silesian University of Technology, ul. Konarskiego 18a, 44-100 Gliwice, Poland

[b] Institute of Materials Science, University of Silesia, ul. Bankowa 12, 40-007 Katowice, Poland

* Corresponding author: E-mail address: rafal.babilas@polsl.pl

Received 22.11.2008; published in revised form 01.01.2009

## ABSTRACT

**Purpose:** The paper presents a microstructure characterization, thermal stability and soft magnetic properties analysis of Fe-based bulk amorphous materials.

**Design/methodology/approach:** The studies were performed on $Fe_{72}B_{20}Si_4Nb_4$ glassy alloy in form of ribbons and rods. The amorphous structure of tested samples was examined by X-ray diffraction (XRD), transmission electron microscopy (TEM) and scanning electron microscopy (SEM) methods. The thermal properties of the glassy samples were measured using differential thermal analysis (DTA) and differential scanning calorimetry (DSC). The magnetic properties were determined by the Maxwell-Wien bridge and VSM methods.

**Findings:** The X-ray diffraction and transmission electron microscopy investigations have revealed that the studied as-cast bulk metallic glasses were amorphous. Broad diffraction halo can be seen for all tested samples, indicating the formation of a glassy phase with the diameters up to 2 mm. The fracture surface of rod samples appears to consist of small fracture zones, which leads to breaking of the samples into parts. A two stage crystallization process was observed for studied amorphous alloy. The changes of crystallization temperatures and magnetic properties as a function of glassy samples thickness were stated.

**Practical implications:** The studied Fe-based alloy system has good glass-forming ability and thermal stability for casting bulk metallic glasses, which exhibit good soft magnetic properties, useful for many electric and magnetic applications.

**Originality/value:** The obtained examination results confirm the utility of applied investigation methods in the microstructure, thermal and soft magnetic properties analysis of examined bulk amorphous alloys.

**Keywords:** Amorphous materials; Bulk metallic glasses; Soft magnetic material; Fe-based alloys

**Reference to this paper should be given in the following way:**

R. Nowosielski, R. Babilas, S. Griner, Z. Stokłosa, Structure and soft magnetic properties of $Fe_{72}B_{20}Si_4Nb_4$ bulk metallic glasses, Archives of Materials Science and Engineering 35/1 (2009) 13-20.

MATERIALS

## 1. Introduction

It is generally known that Fe-based conventional metallic glasses exhibit soft magnetic properties better than the corresponding crystalline alloys. Preparation of that kind of materials requires high critical cooling rates of about $10^6$ K/s.

Inoue et al. found some bulk amorphous alloys, which have good glass-forming ability (GFA) with good soft magnetic

properties in the amorphous state [1-3]. These alloys could be prepared in different form like rods, rings or plates with low critical cooling rates below $10^3$ K/s [4].

Fe-based bulk amorphous alloys with critical cooling rates below $10^3$ K/s have been often found in Fe-based alloy systems containing metalloids (B, C, Si, and P) and early transition elements (Zr, Nb, Hf) [5]. These alloys should realize three Inoue's rules [2] for bulk glass-forming ability: (1) an alloy system consisting of more than three elements, (2) a difference in atomic size ratios above about 12% among the elements, and (3) negative heats of mixing among their elements.

The first Fe-based bulk glassy alloys were prepared in 1995, since then, a variety of Fe-based bulk glassy alloys have been formed and their alloy components can be classified into five groups (Table 1) [6]. The paper presents some results of $Fe_{72}B_{20}Si_4Nb_4$ alloy, which is classified for the IV Group of Fe-based bulk metallic glasses.

Table 1.
Classification of Fe-based bulk metallic glasses [6]

| Group | Examples of Fe-based glassy alloys |
|---|---|
| I. | Fe-(Al,Ga)-(P,C,B,Si)<br>Fe-(Cr,Mo,Nb)-(P,C,B,Si) |
| II. | Fe-(Zr,Hf,Nb,Ta)-B |
| III. | Fe-(Cr,Mo)-(C,B) |
| IV. | Fe-B-Si-Nb<br>Fe-Co-B-Si-Nb<br>Fe-Co-Ni-B-Si-Nb |
| V. | Fe-Nd-Al |

## 2. Materials and research methodology

The aim of the present work is the microstructure characterization, thermal stability and soft magnetic properties analysis of $Fe_{72}B_{20}Si_4Nb_4$ bulk amorphous alloy (Group IV) using XRD, TEM, SEM, DTA, DSC and VSM methods.

The investigated material was cast in form of ribbons with thickness g = of 0.03, 0.08 and 0.20 mm and rods with diameter of $\phi$ = 1.5 and 2 mm. The ribbons were prepared by the continuous casting of the liquid alloy on a copper based wheel. That casting method was applied in works [7-10]. Moreover, rods were manufactured by the pressure die casting. The pressure die casting technique [11] is a method of casting a molten alloy into copper mould under a protective gas pressure (Fig.1).

Structure analysis of studied materials were carried out using X-ray diffraction (XRD). Seifert-FPM XRD 7 diffractometer with $Co_{K\alpha}$ radiation was used for ribbon samples measurements and PANalytical X'Pert diffractometer with $Co_{K\alpha}$ radiation was used for rod samples examination.

Transmission electron microscopy (TEM, TESLA BS 540) was used for the structural characterization of tested glassy samples. Thin foils for TEM observation were prepared by an electrolytic polishing method after a mechanical grinding.

The fracture morphology of studied glassy material in form of rods with diameter of 1.5 and 2 mm was analyzed using the scanning electron microscopy (SEM).

The thermal properties associated with crystallization temperature of the amorphous ribbons were measured using the differential thermal analysis (DTA, Mettler) at a constant heating rate of 6 K/s under an argon protective atmosphere. The differential scanning calorimetry (DSC, Netzsch) was used to determine crystallization and glass transition temperature for tested glassy alloy in form of rods.

The Curie temperature of investigated glassy ribbons was determined by measuring a volume of magnetization in function of temperature. The Curie temperature of amorphous phase was calculated from the condition dM(T)/dT=minimum [12].

The initial magnetic permeability relaxation was measured by using the Maxwell-Wien bridge. Applied magnetic field was a value of 0.5 A/m and frequency about 1 kHz.

The magnetic after effects ($\Delta\mu/\mu$) was determined by measuring changes of magnetic permeability of examined alloys as a function of time after demagnetization, where $\Delta\mu$ is difference between magnetic permeability determined at $t_1$ = 30 s and $t_2$ = 1800 after demagnetization and $\mu$ at $t_1$ [13,14].

The magnetic hysteresis loops of studied metallic glasses were measured by the resonance vibrating sample magnetometer (R-VSM) presented by Wrona et al. [15].

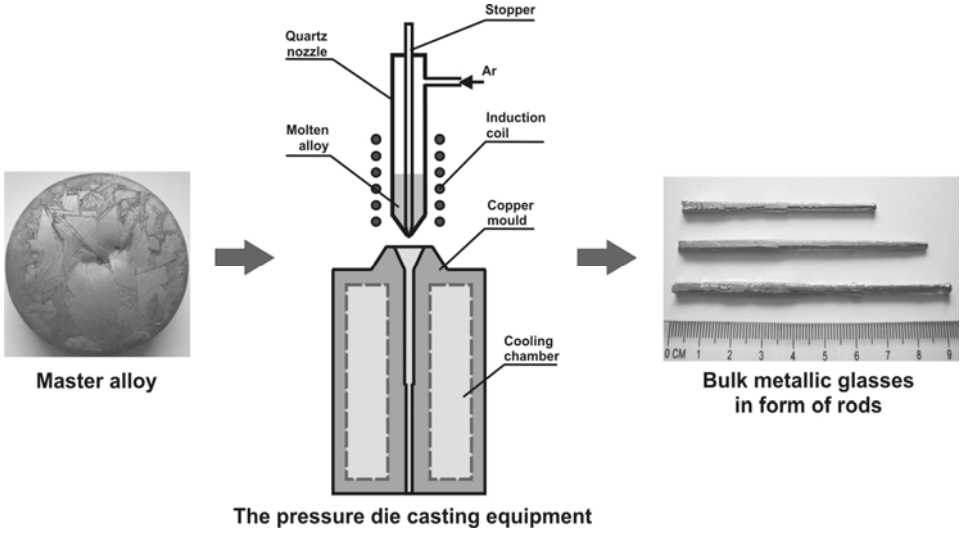


Fig. 1. Schematic illustration of the pressure die casting equipment used for casting bulk amorphous samples [11]

## 3. Results and discussion

The X-ray diffraction investigations have revealed that the studied as-cast bulk metallic glasses were amorphous. The diffraction patterns of tested ribbon samples (Fig.2) and rod samples (Fig.3) have shown the broad diffraction halo characteristic for the amorphous structure.

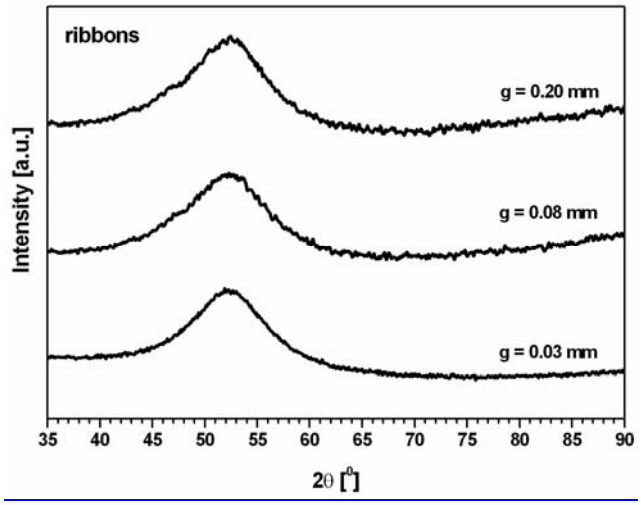


Fig. 2. X-ray diffraction patterns of $Fe_{72}B_{20}Si_4Nb_4$ glassy ribbons in as-cast state with thickness of 0.03, 0.08 and 0.20 mm

Figures 4 and 5 show TEM images and electron diffraction patterns of as-cast ribbon with thickness of 0.03 and 0.2 mm and rod with diameter of 1.5 and 2 mm, adequately.

The TEM images reveal only a changing of contrast and no appreciable contrast corresponding to a crystalline phase is seen. The electron diffraction pattern consists only of halo rings. Broad diffraction halo can be seen for all tested bulk samples, indicating the formation of a glassy phase with the diameters up to 2 mm.

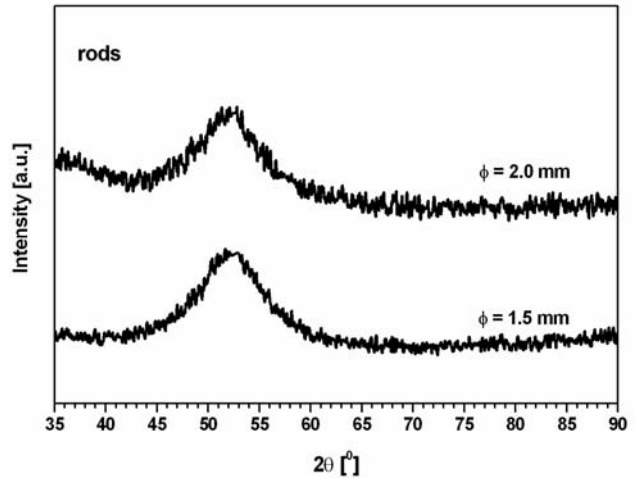


Fig. 3. X-ray diffraction patterns of $Fe_{72}B_{20}Si_4Nb_4$ glassy rods in as-cast state with diameter of 1.5 and 2 mm

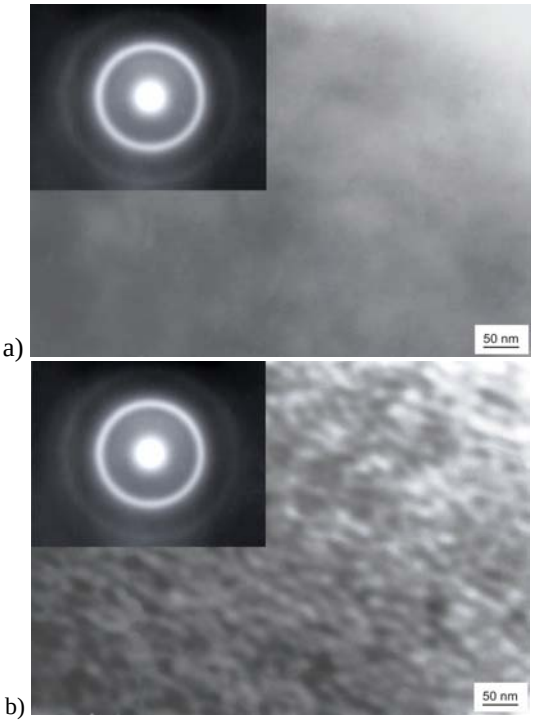


Fig. 4. Transmission electron micrograph and electron diffraction pattern of the as-cast glassy $Fe_{72}B_{20}Si_4Nb_4$ ribbon with a thickness of: (a) 0.03 mm and (b) 0.20 mm

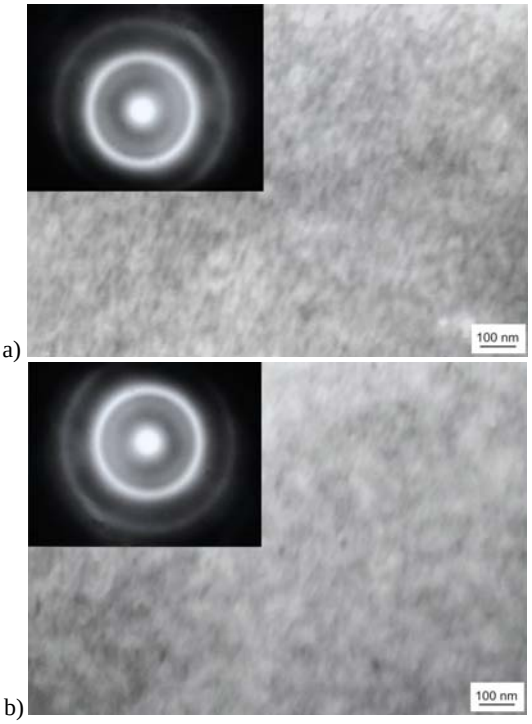


Fig. 5. Transmission electron micrograph and electron diffraction pattern of the as-cast glassy $Fe_{72}B_{20}Si_4Nb_4$ rod with a diameter of: (a) 1.5 mm and (b) 2 mm

a)

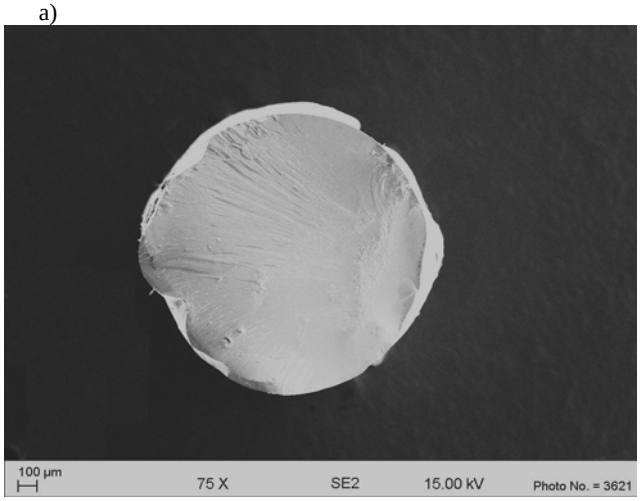


b)

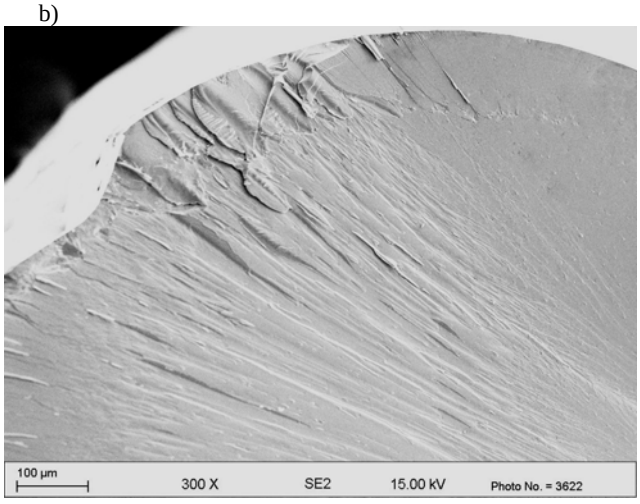


c)

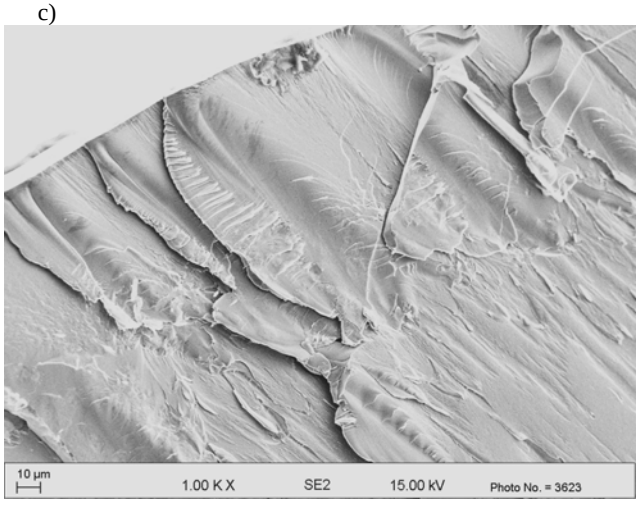


Fig. 6. SEM micrographs of the fracture morphology of $Fe_{72}B_{20}Si_4Nb_4$ amorphous rod in as-cast state with diameter of 1.5 mm

a)

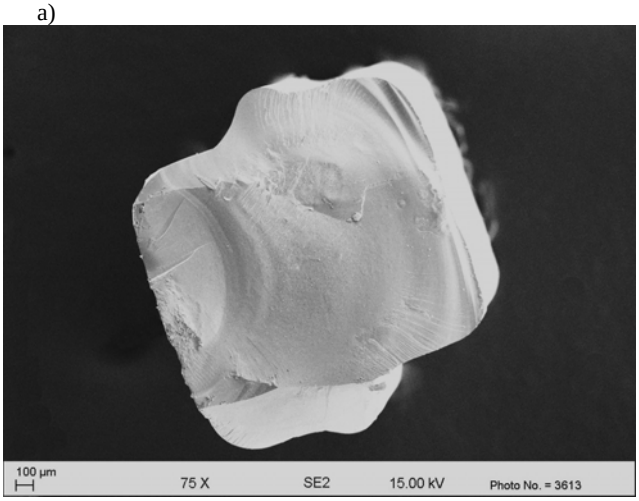


b)

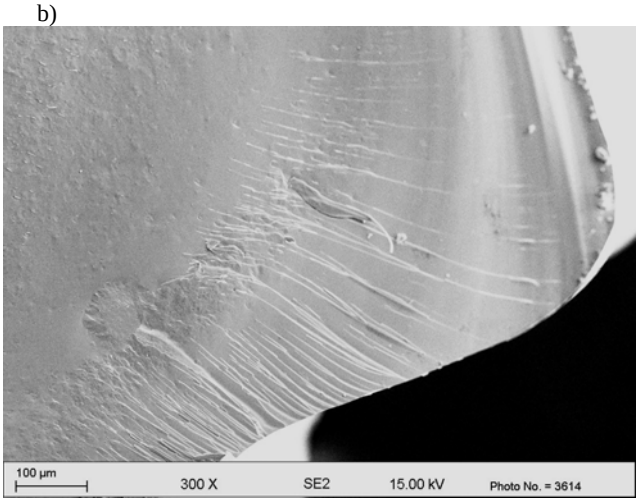


c)

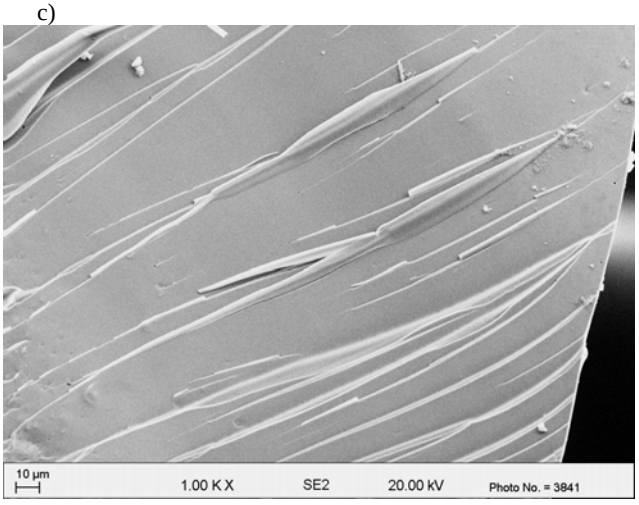


Fig. 7. SEM micrographs of the fracture morphology of $Fe_{72}B_{20}Si_4Nb_4$ amorphous rod in as-cast state with diameter of 2 mm

The appearance of the fracture surface was investigated by SEM method at different magnifications. Figure 6 (a-c) shows micrographs of as-cast glassy rod with diameter of 1.5 mm. What is more, Figure 7 (a-c) presents images of glassy rods with diameter of 2 mm, similarly.

The fracture surface appears to consist of small fracture zones, which leads to breaking of the samples into parts. The presented fractures could be classified as mixed fracture with indicated fluvial fractures, which as characteristic for glassy alloys.

The DTA curves measured on a fully amorphous ribbon samples with thickness of 0.03, 0.08 and 0.20 mm in as-cast state for examined alloy composition are shown in Figure 8.

A two stage crystallization process was observed for $Fe_{72}B_{20}Si_4Nb_4$ bulk amorphous alloy. The exothermic peaks (DTA curves) describing crystallization effects are situated very close. The first stage crystallization of studied glassy alloy for ribbon with thickness of 0.03 mm includes onset crystallization temperature ($T_{x1}$ = 842 K) and peak crystallization temperature ($T_{p1}$ = 864 K). Moreover, analysis of the second crystallization stage allows to determine only peak crystallization temperature ($T_{p2}$ = 892 K), as well.

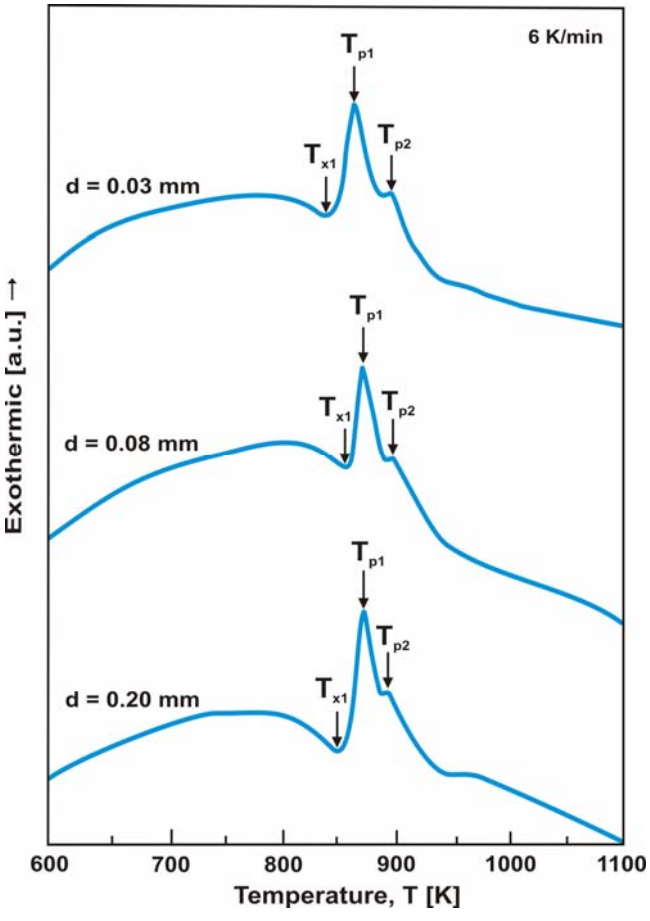


Fig. 8. DTA curves of $Fe_{72}B_{20}Si_4Nb_4$ glassy alloy ribbons in as-cast state

The analysis of crystallization process of tested glassy ribbons shows that crystallization temperature's peak during first stage of crystallization increase with increasing samples thickness and decrease during second stage of crystallization. The differences of crystallization temperature between ribbons with different thickness of the same chemical composition are probably caused by a different degree of relaxation as a result of the different cooling rates during casting process and different amorphous structures of tested glassy samples.

Figure 9 shows normalized magnetization curves as a function of temperature with linear heating rate 5 K/min for examined glassy ribbons. The Curie temperature of amorphous phase of studied ribbons was determined from the dM/dT curves obtained of magnetization data.

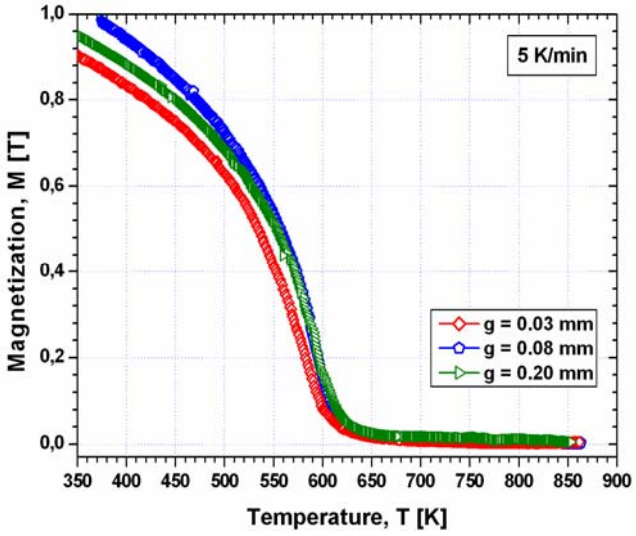


Fig. 9. Normalized curves of magnetization of $Fe_{72}B_{20}Si_4Nb_4$ glassy alloy in form of ribbons in as-cast state

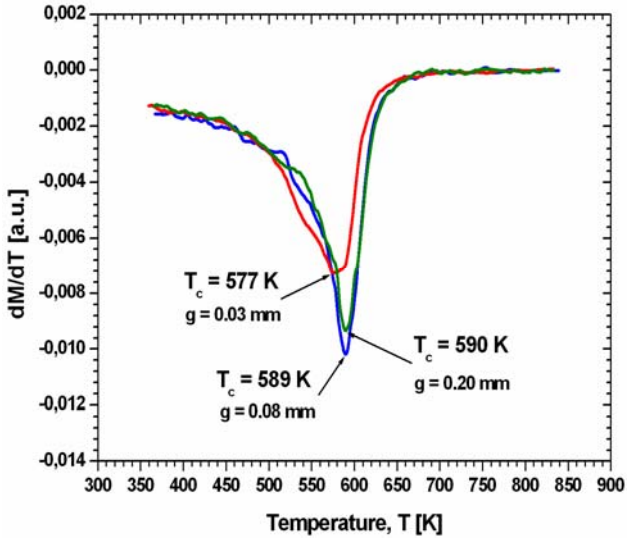


Fig. 10. dM/dT curves versus temperature of as-cast glassy $Fe_{72}B_{20}Si_4Nb_4$ alloy ribbons

Table 2.
Thermal and magnetic properties of $Fe_{72}B_{20}Si_4Nb_4$ bulk metallic glass in form of ribbons

| Alloy | Thickness [mm] | Thermal properties | | | Magnetic properties | | | |
|---|---|---|---|---|---|---|---|---|
| | | $T_c$ [K] | $T_{p1}$ [K] | $T_{p2}$ [K] | $B_s$ [T] | $H_c$ [A/m] | $\mu_r$ | $\Delta\mu/\mu$ [%] |
| $Fe_{72}B_{20}Si_4Nb_4$ | 0.03 | 577 | 864 | 892 | 1.04 | 8.0 | 1293 | 9.4 |
| | 0.08 | 589 | 869 | 893 | 1.12 | 4.8 | 2209 | 4.9 |
| | 0.20 | 590 | 871 | 890 | 1.11 | 5.6 | 2527 | 3.0 |

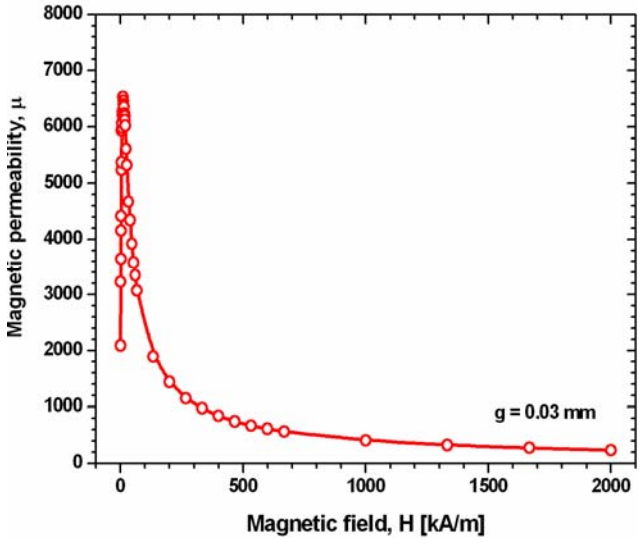


Fig. 11. Maximum magnetic permeability of $Fe_{72}B_{20}Si_4Nb_4$ glassy ribbon in as-cast state with thickness of 0.03 mm

The Curie temperature ($T_c$) for sample with thickness of 0.03 mm has a value of 577 K, for ribbon with thickness of 0.08 mm $T_c$ = 589 K and $T_c$ has a value of 590 K for sample with thickness of 0.20 mm (Fig.10). A variation of the Curie temperature is probably also due to a more relaxed amorphous structure of the tested ribbons with increasing thickness.

The crystallization temperatures obtained from DTA curves and Curie temperature determined from normalized curves of magnetization are connected with thermal properties of studied metallic glasses in as-cast state.

The initial magnetic permeability ($\mu_r$) of $Fe_{72}B_{20}Si_4Nb_4$ is 1293 for ribbon with thickness of 0.03 mm and $\mu_r$ = 2527 for sample with thickness of 0.20 mm. Moreover, the initial magnetic permeability of studied alloy cast in form of rods has a lower value, $\mu_r$ = 426 for sample with diameter of 1.5 and $\mu_r$ = 161 for rod with diameter of 2 mm.

In addition, Figure 11 presents curve of maximum magnetic permeability ($\mu_{max}$ = 6500) obtained for glassy ribbon in as-cast state with thickness of 0,03 mm.

From magnetic hysteresis loops obtained from VSM measurements of investigated materials, coercive field and magnetic saturation induction was determined (Fig.12).

The coercive field ($H_c$) of tested metallic glasses has a value of 8.8 A/m for glassy ribbon with thickness of 0.03 mm and $H_c$ = 7.2 A/m for sample with thickness of 0.20 mm. What is more, the coercive field has a value of 11 A/m for rod with diameter of 1.5 mm and $H_c$ = 55 A/m for rod with diameter of 2 mm. The saturation induction ($B_s$) of studied glassy ribbon has a value of 0.77 T and 0.72 T for samples with thickness of 0.03 and 0.20 mm, adequately.

The DSC examinations of rod samples allow to determine the peak crystallization temperature: $T_{p1}$ = 860 K for sample with diameter of 1.5 mm and $T_{p1}$ = 865 K for sample with diameter of 2 mm. The glass transition temperature ($T_g$ = 810 K for diameter of 1.5 mm, $T_g$ = 812 K for diameter of 2 mm) was determined as well.

The magnetic permeability relaxation ($\Delta\mu/\mu$), which was determined for samples with thickness of 0.03, 0.08 and 0.20 mm has a value of 9.4, 4.9 and 3.0 %. Moreover, ($\Delta\mu/\mu$) has value of 1.4 and 0.9 % for rods with diameter of 1.5 and 2 mm.

Figure 13 presents magnetic after effects ($\Delta\mu/\mu$) determined at room temperature versus sample thickness for glassy ribbons and rods in as-cast state.

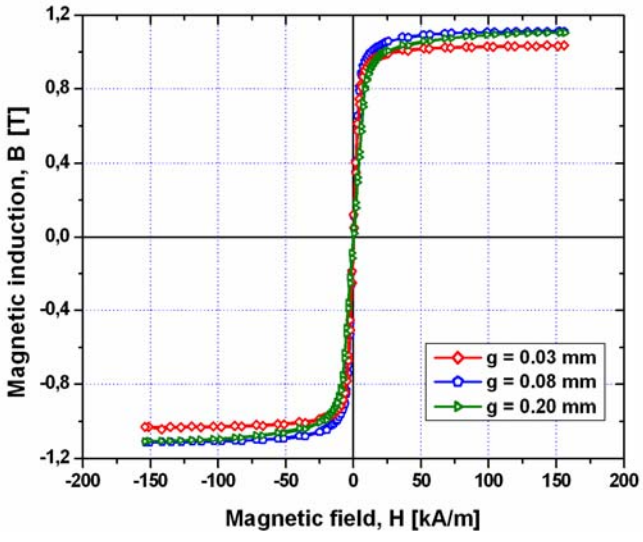


Fig. 12. Hysteresis loops of tasted $Fe_{72}B_{20}Si_4Nb_4$ glassy alloy ribbons with thickness of 0.03, 0.08 and 0.02 mm

Table 3.
Thermal and magnetic properties of $Fe_{72}B_{20}Si_4Nb_4$ bulk metallic glass in form of rods

| Alloy | Thickness [mm] | Thermal properties | | | Magnetic properties | | |
|---|---|---|---|---|---|---|---|
| | | $T_g$ [K] | $T_{p1}$ [K] | $T_{p2}$ [K] | $H_c$ [A/m] | $\mu_r$ | $\Delta\mu/\mu$ [%] |
| $Fe_{72}B_{20}Si_4Nb_4$ | 1.5 | 810 | 860 | 952 | 11 | 426 | 1.4 |
| | 2.0 | 812 | 865 | 952 | 55 | 161 | 0.9 |

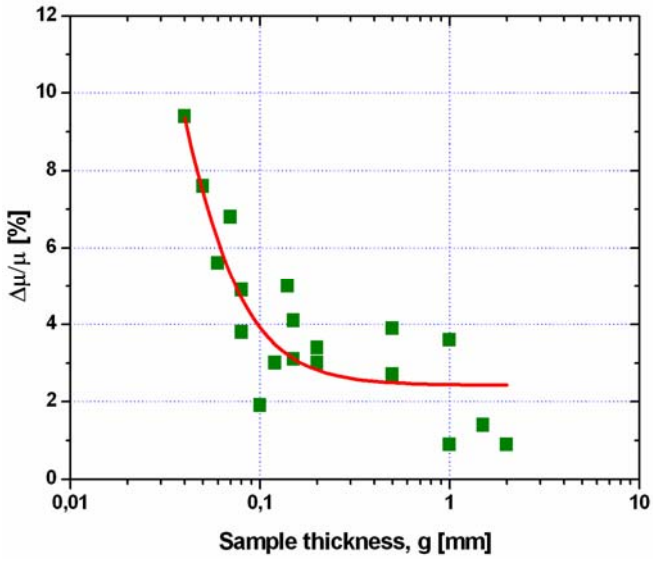


Fig. 13. The magnetic permeability relaxation ($\Delta\mu/\mu$) determined at room temperature versus sample thickness

$\Delta\mu/\mu$ is directly proportional to the concentration of defects in amorphous materials, i.e. microvoids concentration. It is obvious that value of magnetic permeability relaxation decrease with increasing sample thickness. That result has also probably corresponds with a variation of crystallization temperatures and soft magnetic properties of studied glassy material.

Table 2 and 3 also give information about thermal and magnetic properties of studied amorphous alloys in form of ribbon and rods. The obtained results of structure, thermal and magnetic properties allow to classify the studied Fe-based glassy alloy for suitable material for electric and magnetic applications.

## 4. Conclusions

The investigations performed on the samples of $Fe_{72}B_{20}Si_4Nb_4$ bulk metallic glass allowed to formulate the following statements:

- the X-ray diffraction and transmission electron microscopy investigations have revealed that the studied as-cast bulk metallic glasses were amorphous,
- the TEM images reveal only a changing of contrast and no appreciable contrast corresponding to a crystalline phase is seen,
- the SEM images show that studied fractures could be classified as mixed fracture with indicated fluvial fractures, which as characteristic for glassy metals,
- a two stage crystallization process was observed for studied bulk amorphous alloy,
- changes of Curie temperatures, crystallization temperatures and magnetic properties as a function of glassy ribbons thickness (time of solidification) were stated,
- the magnetic permeability relaxation ($\Delta\mu/\mu$), which is directly proportional to the microvoids concentration in amorphous structure decrease with increasing sample thickness,
- the investigated thermal and magnetic properties allow to classify the studied bulk metallic glasses as suitable materials for electric and magnetic applications.

## Acknowledgements

The authors would like to thank Dr A. Zajączkowski, Mr W. Głuchowski (Non-Ferrous Metals Institute, Gliwice) and Mr W. Skowroński (Department of Electronics, AGH University of Science and Technology, Kraków) for a cooperation.

This work is supported by Polish Ministry of Science (grant N507 027 31/0661).

## References

[1] A. Inoue, K. Hashimoto, Amorphous and nanocrystalline materials: preparation, properties and applications, Springer, 2001.
[2] A. Inoue, Bulk amorphous and nanocrystalline alloys with high functional properties, Materials Science and Engineering A304-306 (2001) 1-10.
[3] A. Inoue, A. Makino, T. Mizushima, Ferromagnetic bulk glassy alloys, Journal of Magnetism and Magnetic Materials 215-216 (2000) 246-252.
[4] R. Nowosielski, R. Babilas, Fabrication of bulk metallic glasses by centrifugal casting method, Journal of Achievements in Materials and Manufacturing Engineering, 20 (2007) 487-490.
[5] R. Nowosielski, R. Babilas, P. Ochin, Z. Stokłosa, Thermal and magnetic properties of selected Fe-based metallic glasses, Archives of Materials Science and Engineering, 30/1 (2008) 13-16.

[6] A. Inoue, B.L. Shen, C.T. Chang, Fe- and Co-based bulk glassy alloys with ultrahigh strength of over 4000 MPa, Intermetallics 14 (2006) 936-944.
[7] D. Szewieczek, J. Tyrlik-Held, S. Lesz, Structure and mechanical properties of amorphous $Fe_{84}Nb_7B_9$ alloy during crystallization, Journal of Achievements in Materials and Manufacturing Engineering 24/1 (2007) 87-90.
[8] D. Szewieczek, T. Raszka, J. Olszewski, Optimisation the magnetic properties of the $(Fe_{1-x}Co_x)_{73.5}Cu_1Nb_3Si_{13.5}B_9$ (x=10; 30; 40) alloys, Journal of Achievements in Materials and Manufacturing Engineering 20 (2007) 31-36.
[9] S. Lesz, D. Szewieczek, J.E. Frąckowiak, Structure and magnetic properties of amorphous and nanocrystalline $Fe_{85.4}Hf_{1.4}B_{13.2}$ alloy, Journal of Achievements in Materials and Manufacturing Engineering 19 (2006) 29-34.
[10] S. Lesz, D. Szewieczek, J. Tyrlik-Held, Correlation between fracture morphology and mechanical properties of NANOPERM alloys, Archives of Materials Science and Engineering 29/2 (2008) 73-80.
[11] R. Nowosielski, R. Babilas, Structure and magnetic properties of $Fe_{36}Co_{36}B_{19}Si_5Nb_4$ bulk metallic glasses, Journal of Achievements in Materials and Manufacturing Engineering 30/2 (2008) 135-140.
[12] Z. Stokłosa, J. Rasek, P. Kwapuliński, G. Haneczok, G. Badura, J. Lelątko, Nanocrystallisation of amorphous alloys based on iron, Materials Science and Engineering C 23 (2003) 49-53.
[13] P. Kwapuliński, J. Rasek, Z. Stokłosa, G. Haneczok, Magnetic properties of $Fe_{74}Cu_1Cr_xZr_{3-x}Si_{13}B_9$ amorphous alloys, Journal of Magnetism and Magnetic Materials 254–255 (2003) 413-415.
[14] P. Kwapuliński, Z. Stokłosa, J. Rasek, G. Badura, G. Haneczok, L. Pająk, L. Lelątko, Influence of alloying additions and annealing time on magnetic properties in amorphous alloys based on iron, Journal of Magnetism and Magnetic Materials 320 (2008) 778-782.
[15] J. Wrona, M. Czapkiewicz, T. Stobiecki, Magnetometer for the measurements of the hysteresis loop of ultrathin magnetic layers, Journal of Magnetism and Magnetic Materials 196 (1999) 935-936.